Protein Science (1996), 5:1942–1946. Cambridge University Press. Printed in the USA.

FOR THE RECORD

A fragment of staphylococcal nuclease with an OB-fold structure shows hydrogen-exchange protection factors in the range reported for "molten globules"

ANDREI T. ALEXANDRESCU, SONJA A. DAMES, AND RONALD WILTSCHECK

Department of Structural Biology, Biozentrum, University of Basel, Basel, Switzerland, CH-4056

(RECEIVED May 16, 1996; ACCEPTED June 21, 1996)

Abstract: Hydrogen-exchange rates for an OB-fold subdomain fragment of staphylococcal nuclease have been measured at pH 4.7 and 4 °C, conditions close to the minimum of acid/base catalyzed exchange. The strongest protection from solvent exchange is observed for residues from a five-stranded β-barrel in the NMR structure of the protein. Protection factors, calculated from the experimental hydrogen-exchange rates, range between 1 and 190. Similarly small protection factors have in many cases been attributed to "molten globule" conformations that are supposed to lack a specific tertiary structure. The present results suggest that marginal protection from solvent exchange does not exclude well-defined structure.

Keywords: hydrogen exchange; kinetic intermediate; molten globule; NMR structure; protection factors; protein folding

A common application of hydrogen-exchange methodology is the characterization of species that are not amenable to direct NMR study. These include short-lived kinetic folding intermediates (Roder et al., 1988; Udgaonkar & Baldwin, 1988), equilibrium folding intermediates with large line-broadening contributions due to conformational exchange or aggregation (Hughson et al., 1990) protein–chaperone complexes that are otherwise too large for NMR analysis (Zahn et al., 1994), and subglobal unfolding units whose concentrations are too small to allow direct NMR detection (Bai et al., 1995). Hydrogen-exchange data are usually analyzed in terms of the Linderstrøm-Lang (1955) model. This model presupposes a "closed" exchange resistant conformation, and an "open" exchange susceptible conformation for each labile site:

$$\text{closed} \underset{k_{cl}}{\overset{k_{op}}{\rightleftarrows}} \text{open} \xrightarrow{k_{ch}} \text{exchanged}. \quad (1)$$

Exchange is believed to occur due to transient "breaking" of hydrogen bonds, through either local or global fluctuations in protein structure. In the *EX1* limit, the rate of closing (k_{cl}) is much slower than the intrinsic "chemical" rate of exchange (k_{ch}), and the observed rate (k_{obs}) is limited by the opening rate (k_{op}):

$$k_{obs} = k_{op}\ (k_{cl} \ll k_{ch}). \quad (2)$$

In the *EX2* limit, k_{cl} is much faster than k_{ch}, and k_{obs} is limited by the fraction of conformations in the *open* state:

$$k_{obs} = \frac{k_{op}}{k_{cl}} \cdot k_{ch}\ (k_{ch} \ll k_{cl}). \quad (3)$$

In the *EX1* limit, hydrogen exchange is pH-independent, whereas in the *EX2* limit, k_{ch} and hence k_{obs} increase 10-fold with each pH unit (Baldwin, 1993). The *EX2* limit is almost always observed in the pH range between 4 and 7 (Bai et al., 1995) because formation of hydrogen-bonded structure is usually much faster than intrinsic exchange (Englander & Kallenbach, 1984). In kinetic experiments, where pH values ranging between 9 and 11 are often necessary to achieve hydrogen-exchange timescales (~1 ms) comparable to those for protein folding or unfolding (Baldwin, 1993), hydrogen exchange may be in the *EX1* regime (Englander & Mayne, 1992) or in the range between the *EX1* and *EX2* limits (Pedersen et al., 1993). The pH dependence of k_{obs} can be used to distinguish between *EX1* and *EX2* mechanisms, provided k_{cl} and k_{op} are invariant as a function of pH (Pedersen et al., 1993).

It is possible to correct k_{obs} for the effects of pH, temperature, and protein sequence (to a first approximation nearest neighbor effects) by normalizing against exchange rates for model peptides (k_{mod}). In the *EX2* limit, with the assumption $k_{ch} \sim k_{mod}$, Equation 3 can be recast to a form that describes an equilibrium constant relating the concentrations of open and closed conformations:

$$\frac{k_{obs}}{k_{mod}} \cong \frac{k_{op}}{k_{cl}} = \frac{[\text{open}]}{[\text{closed}]} = K_{op},$$

$$\Delta G_{op} = -RT \ln K_{op}. \quad (4)$$

Reprint requests to: Andrei T. Alexandrescu, Department of Structural Biology, Biozentrum, University of Basel, Klingelbergstrasse 70, Basel, Switzerland, CH-4056.

Abbreviations: $\Delta G_u(0)$, free-energy of unfolding extrapolated to zero denaturant concentration; GuHCl, guanidinium hydrochloride; HSQC, heteronuclear single quantum correlation; OB-fold, oligonucleotide/oligosaccharide-binding fold; pdTp, thymidine 3′,5′-bisphosphate; PF, protection factor; SN-OB, residues 1–103 fragment of staphylococcal nuclease containing the global suppressor mutations V66L and G88V.

The reciprocal of the equilibrium constant K_{op} is commonly expressed as a "protection factor" (PF $\cong 1/K_{op}$) that describes the slowing of hydrogen exchange relative to model peptides. In the *EX2* limit, the protection factor is thus specifically a measure of the stability of a given hydrogen bonded site.

SN-OB is a 1–103 fragment of the 149-residue protein staphylococcal nuclease that contains the global suppressor mutations V66L and G88V (Shortle & Meeker, 1989; Alexandrescu et al., 1995). These mutations were identified as second-site revertants of mutant nuclease phenotypes using assays of enzymatic activity (Shortle, 1986), and stability to denaturation (Shortle & Meeker, 1986). The NMR structure of SN-OB has been solved based on NOE-distance and $^3J_{HNH\alpha}$-dihedral restraints (Alexandrescu et al., 1995). The structure consists of the "OB-fold" (Murzin, 1993) subdomain of wild-type nuclease: a five-stranded β-barrel and an α-helix. When SN-OB is dissolved in D_2O under the conditions for which the NMR structure was determined (pH 4.7, 32 °C), all labile amide protons are exchanged in less than 20 min. To obtain quantitative data, we measured hydrogen-exchange rates for SN-OB at pH 4.7 and 4 °C. Under these conditions, most amide protons with protection factors greater than 10 should persist long enough (~30 min) to allow detection of their NMR signals in D_2O.

Results and discussion: Figure 1A shows ^1H-^{15}N HSQC spectra of SN-OB in H_2O; and as a function of time after dissolving the protein in D_2O (Fig. 1B,C,D). Figure 2 shows protection factors calculated from the hydrogen-exchange data by the method of Bai et al. (1993), mapped on to the sequence (Fig. 2A) and NMR structure (Fig. 2B) of SN-OB. To a first approximation, the amide protons that are most resistant to solvent exchange are from residues in the five-stranded β-sheet and the α-helix of SN-OB.

Figure 3 shows GuHCl denaturation profiles for SN-OB monitored by mean residue ellipticity at 221 and 275 nm. The denaturation curves give $\Delta G_u(0)$ values of 2.4 ± 0.5 kcal/mol and 1.9 ± 0.4 kcal/mol for the peptide (Fig. 3A) and aromatic (Fig. 3B) regions of the CD spectrum, respectively. The $\Delta G_u(0)$ value obtained

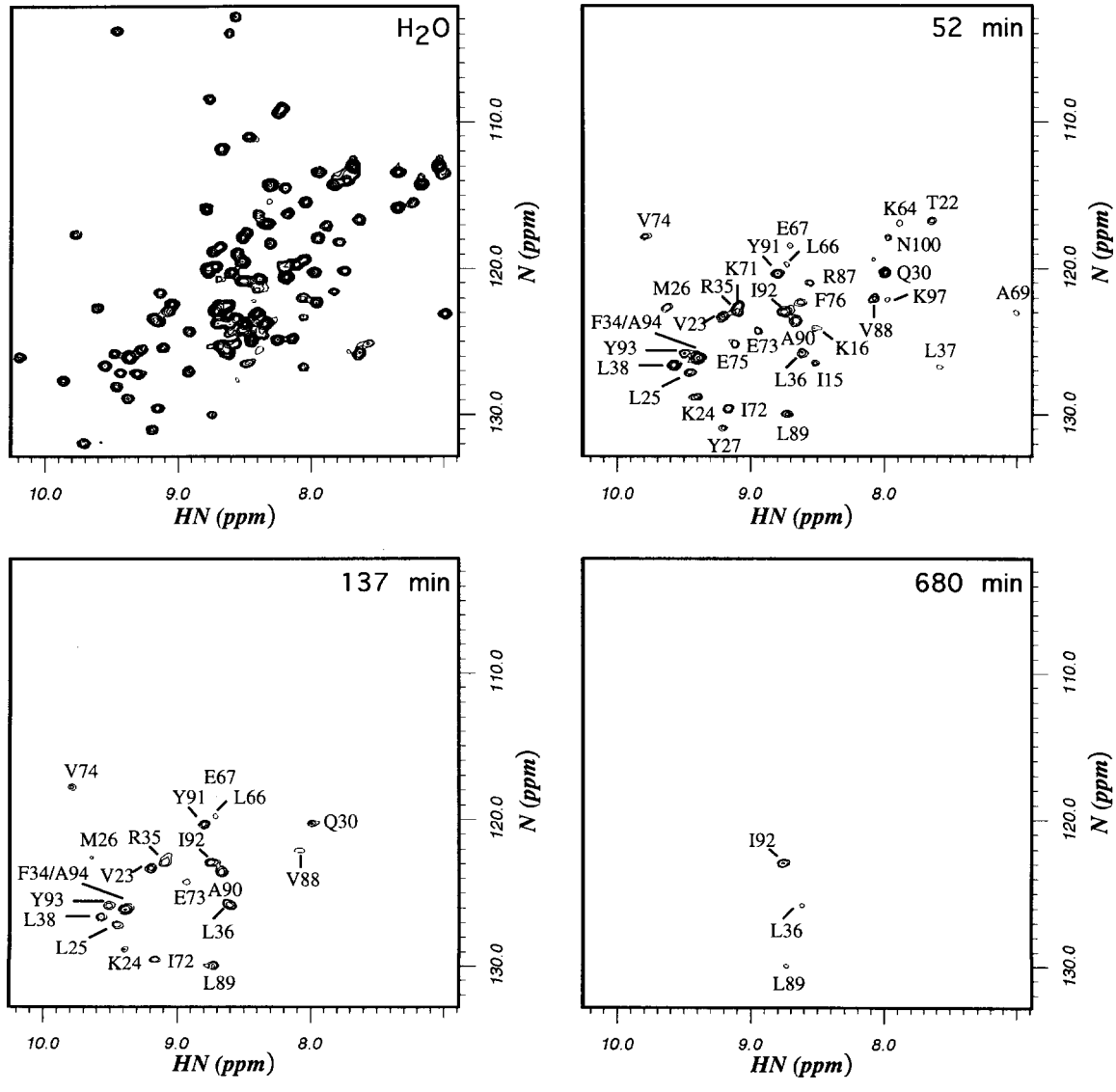

Fig. 1. Gradient ^1H-^{15}N HSQC spectra of 1.4 mM SN-OB in 90% H_2O/10% D_2O (**A**), and after exchange in D_2O for the times indicated (**B**, **C**, **D**).

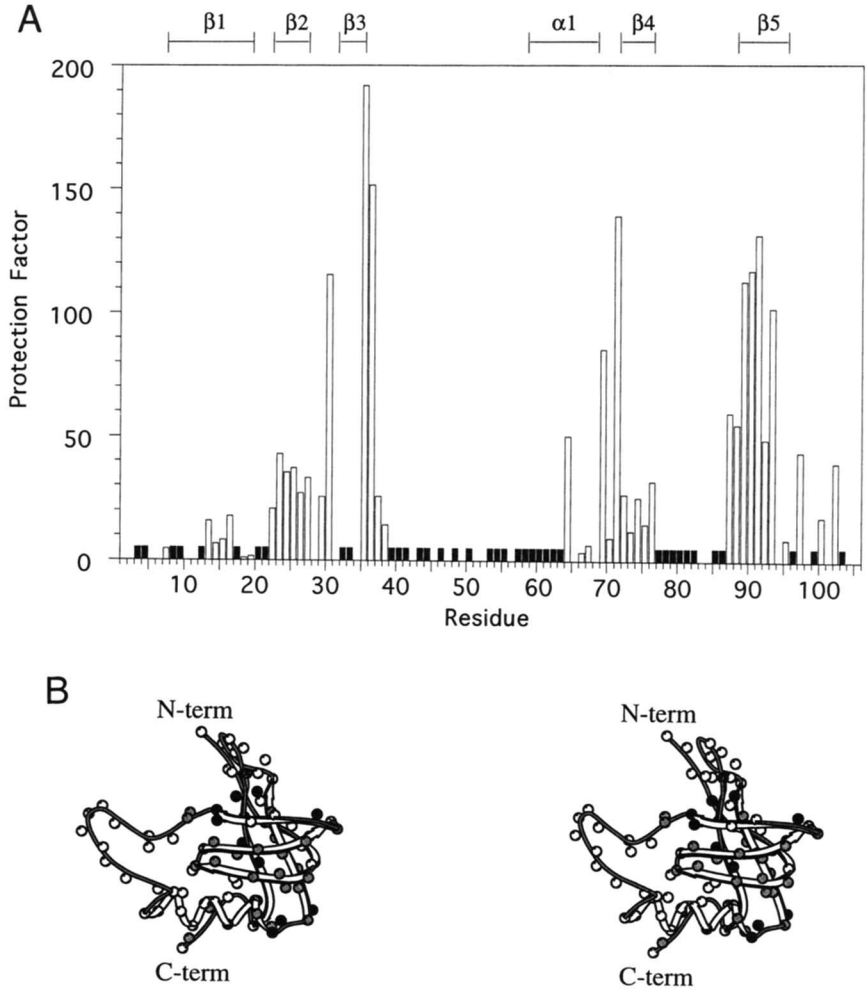

Fig. 2. Protection factors for SN-OB. **A:** Protection factors as a function of sequence. Black bars indicate amide protons that exchanged too fast to allow quantitative determination of hydrogen-exchange rates. **B:** Protection factors as a function of the NMR structure of SN-OB (Alexandrescu et al., 1995; lowest energy NMR structure of PDB accession code 2SOB). White circles, fast exchangers; gray, protection factors between 1 and 50; black, protection factors above 50. The fastest experimentally determined rate was 0.0016 s^{-1} for residue I18. Excluding the N-terminus, the fastest intrinsic rate predicted for SN-OB is 0.055 s^{-1} for residue E101. Based on these observations, it is possible to estimate an upper limit of 34 on the protection factors of any residues indicated by black bars in A or white circles in B.

from the peptide region of the CD spectrum predicts protection factors ranging from 30 to 190 for amide protons that exchange through a global unfolding mechanism (Equation 4), consistent with the hydrogen-exchange data (Fig 2A). The highest protection factors in SN-OB are reduced by factors of 300 and 5,000 compared to those of wild-type nuclease, and to those for the protein complexed with the inhibitor pdTp (Loh et al., 1993), respectively. The attenuated protection from solvent-exchange in SN-OB is consistent with the lower free energy of unfolding for this protein, compared to that for wild-type nuclease [$\Delta G_u(0) = 6.4 \pm 0.3$ kcal/mol, 37 °C], and to that for wild-type nuclease complexed with pdTp [$\Delta G_u(0) = 8.2 \pm 0.3$ kcal/mol, 37 °C] (Loh et al., 1993).

Protection factors for SN-OB fall between 1 (I18 in β1) and 190 (R35 in β3). Similarly low protection from solvent exchange has often been attributed to unstructured, and/or "molten globule" conformations (Hughson et al., 1990; Miranker et al., 1991; Englander & Mayne, 1992; Lu & Dahlquist, 1992; Radford et al., 1992; Baldwin, 1993; Robinson et al., 1994; Zahn et al., 1994; Miranker & Dobson, 1996). For example, a kinetic intermediate of a P117G mutant of staphylococcal nuclease shows protection factors ranging between 1 and 63 (Jacobs & Fox, 1994). The strongest protection in this kinetic intermediate occurs for regions of the polypeptide chain that form the β-sheet of wild-type nuclease, and of SN-OB. It has been suggested (Jacobs & Fox, 1994) that the β-sheets comprised of strands 1–3 and 4–5 may only be associated through "molten hydrophobic interactions" in this kinetic intermediate. The basis for this suggestion was the lack of significant protection for the two "tertiary" amide proton probes of A12 (PF = 2) and A90 (PF = 6), which in the X-ray structure of wild-type nuclease are hydrogen bonded to the carbonyls of I72 and R35, respectively. In the present study, A90 has a protection factor of 117, whereas the exchange rate of A12 is too fast to measure (we estimate an upper bound of 3 on the protection factor for A12). In general, there is a good correlation between protection from hydrogen exchange and hydrogen bonds observed in crystallographic studies (Englander & Mayne, 1992). It is not too uncommon, however, to find that amide protons that are hydrogen bonded in a crystal structure show only marginal protection from exchange. This fast exchange presumably reflects that local hydrogen bond stability is lower than that for global unfolding. For the kinetic intermediate of nuclease P117G, the low protection of the amide protons of A12 and A90 may reflect that the β-barrel structure is not formed (Jacobs & Fox, 1994). Alternatively, the β-barrel may be formed, and the fast exchange of the two amide protons could reflect a lower stability for the tertiary A12-I72 and R35-A90 hydrogen bonds than that for global unfolding.

In its original definition (Dolgikh et al., 1981; Ohgushi & Wada, 1983), the molten globule is a compact conformation with a native-like secondary structure, but a fluctuating tertiary structure. Examples were given for the molten globules of α-lactalbumin

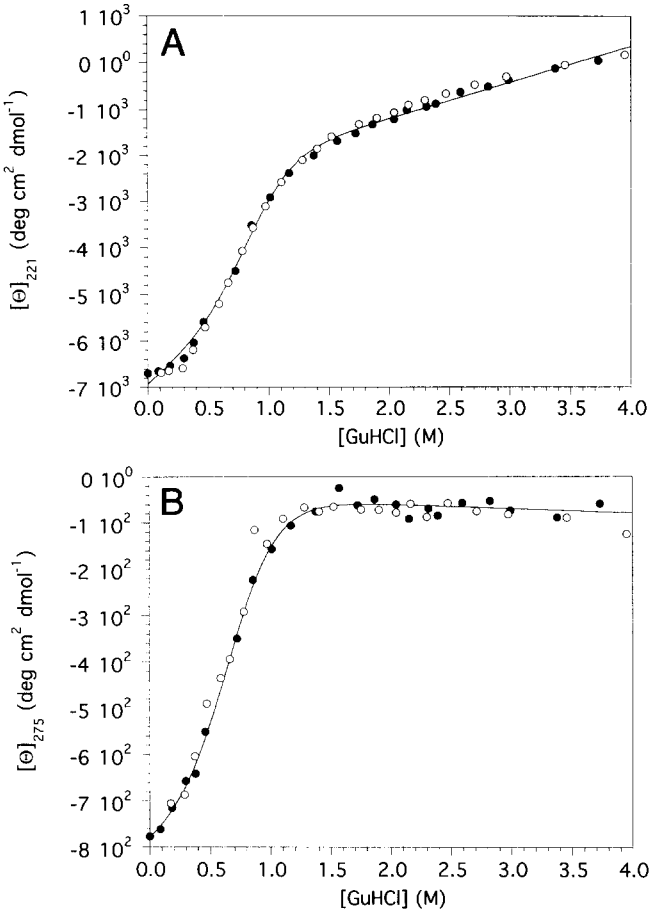

Fig. 3. Mean residue ellipticity of SN-OB at 221 nm (**A**) and 275 nm (**B**) as a function of GuHCl concentration (filled circles, F → U transition; open circles, U → F transition). Lines represent six-parameter nonlinear least-squares fits (Kalnin & Kuwajima, 1995) of the F → U transitions to a two-state unfolding model. The U → F data are shown for reference but were not included in the fit because there are fewer points to define the folded-state baseline. The parameters obtained for the unfolding transitions are C_m = 0.87 ± 0.09 M, m = 2.8 ± 0.5 kcal•mol^{-1}•M^{-1} for the 221 nm data; C_m = 0.69 ± 0.10 M, m = 2.8 ± 0.4 kcal•mol^{-1}•M^{-1} for the 275 nm data. $\Delta G_u(0)$ values of 2.4 ± 0.5 kcal•mol^{-1} and 1.9 ± 0.4 kcal•mol^{-1} were calculated for the 221 nm and 275 nm data, respectively, by solving the equation $\Delta G_u = m(c_M - c)$ for zero denaturant concentration.

(Dolgikh et al., 1981) and of cytochrome *c* (Ohgushi & Wada, 1983). For both molten globules, the NMR chemical shift dispersion was considerably smaller than that of the respective native states, and approached that of a random coil conformation. The NMR data for SN-OB are clearly inconsistent with a molten globule conformation. The NMR structure of SN-OB (Alexandrescu et al., 1995; PDB accession code 2SOB) is based on 265 long-range NOE constraints. The β-barrel of SN-OB (residues 7-1-8, 22–35, 71–76, 88–95) is reasonably well defined (Cα,N,C′ RMSD of 0.72 Å between NMR structures), and highly similar to that in the X-ray structure (Hynes & Fox, 1991) of wild-type nuclease (Cα,N,C′ RMSD of 1.13 Å). The NMR structure of SN-OB was determined at 32 °C, and the hydrogen-exchange data were collected at 4 °C. Amide proton chemical shift values range between 7.09 ppm (A69) and 10.21 ppm (K70) at 32 °C (Alexandrescu et al., 1995), and between 6.98 ppm (A69) and 10.19 ppm (K70) at 4 °C (Fig. 1A). By contrast, amide proton chemical shift values for residues 1–103 in nuclease under strongly denaturing conditions (Wang & Shortle, 1995) range from 7.9 ppm (E57) to 8.7 ppm (I92). The NMR chemical shift dispersion at 4 °C indicates that the protein contains significant tertiary structure. Furthermore, all amide proton chemical shifts are conserved within ±0.24 ppm between the two temperatures. Considering the relatively high sensitivity of amide proton chemical shifts to temperature, changes of this magnitude suggest that the structure of SN-OB is highly conserved between the two temperatures. Indeed, we estimate an upper limit of 500 on the protection factors for any of the backbone amide protons of SN-OB under the conditions (pH 4.7, 32 °C) for which the NMR structure was determined [based on the observation that all amide protons exchange within 20 min of dissolving the protein in D_2O ($k_{obs} > 0.0008$ s^{-1}), the exclusion of the fastest exchanging amide protons with k_{obs} between 0.1 s^{-1} and 10 s^{-1} in magnetization transfer experiments (data not shown), and the consideration of the highest remaining k_{mod} rate (0.42 s^{-1} for G29)]. In addition to SN-OB, we are aware of at least two other proteins, rTAP (Antuch et al., 1994) and apo-calmodulin (Kuboniwa et al., 1995; Tjandra et al., 1995), with well-defined NMR structures that offer only marginal protection from solvent exchange.

The timescale of the NOE is on the order of nanoseconds (Neri et al., 1992), a timescale considerably faster than that of hydrogen-exchange experiments (Baldwin, 1995). Conformations that are stable on the timescale of the NOE, or on the timescales of spectroscopic techniques such as CD or IR, may interconvert with exchange-susceptible conformations on timescales much faster than those of hydrogen-exchange experiments (Buck et al., 1994; Guijarro et al., 1995). Furthermore, because the NOE decays with the inverse sixth power of the distance between two protons, the time-averaged intensity of the NOE will be dominated by those conformations that achieve interproton distances shorter than 5 Å. Indeed, it has been estimated that long-range NOE effects can arise from a fractional population of folded molecules as low as 0.1 (Neri et al., 1992). Conversely, unfolded conformations of a protein with a fractional population much below 0.1 would not be easily detectable in an NMR spectrum (Bai et al., 1995). Estimates of the accuracy of protection factors suggest that measured values may differ by factors of 2–5 from true values, due to systematic errors in k_{mod} rates (Buck et al., 1994; Koide et al., 1995). Taken together, these observations suggest that, in principle, a protection factor as low as unity may not rule out structure that is either marginally stable on the timescales of hydrogen exchange, or significantly stable on timescales faster than those of hydrogen exchange.

Protection from solvent exchange is strictly a function of the dynamics and stability of hydrogen-bonded conformations (Equations 1–4). In the absence of high-resolution structural data, conclusions about the type and extent of structure responsible for hydrogen-exchange behavior may be unwarranted.

Materials and methods: ^{15}N-labeled SN-OB was prepared as described previously (Shortle & Meeker, 1989; Alexandrescu et al., 1995). Hydrogen exchange was initiated by dissolving a fresh sample of ^{15}N-labeled SN-OB in a 99.99% D_2O solution of 50 mM acetate, pH 4.5. The final pH of the sample measured after completion of the hydrogen-exchange experiment was 4.7. NMR data were recorded on a Varian *Unity*+ 600 MHz NMR machine, with the NMR probe thermostated to temperature of 4 °C. Twenty-nine ^{1}H-^{15}N gradient-HSQC spectra (Kay et al., 1992) with 1,024 ^{1}H and 75 ^{15}N complex points were collected over a total period of 1,058 min. The 4 earliest time points were collected with 1 scan

per FID (3 min per HSQC experiment). For the next 16 time points, 4 transients were averaged per FID (12 min per HSQC experiment). For the last 9 time points, 16 transients were averaged per FID (47 min per HSQC experiment). The dead time of the hydrogen-exchange experiment was 17 min. Of this, the slowest step was the time required to dissolve SN-OB at 4 °C.

The normalized intensity maximum of each cross-peak in the HSQC spectra was measured as a function of exchange time, defined as the period from the addition of D_2O/acetate buffer to a lyophilized SN-OB sample to the end of each HSQC experiment. Rate constants for exchange were obtained from a nonlinear least-squares fit of the exponential decay data to the equation (Bai et al., 1993):

$$H = H_o \exp(-k_{obs}t) + C$$

with the initial intensity H_o, the baseline C, and the observed exchange rate k_{obs}, as free variables in the fit. Protection factors were calculated from the observed exchange rates and the k_{mod} rates of Bai et al. (1993).

CD data were collected on a Jasco J720 spectropolarimeter. A 0.1-cm cuvette was used for measurements at 221 nm, and a 1-cm cuvette for measurements at 275 nm. Cuvettes were thermostated at 4 °C during measurements. For the unfolding transitions, 37.5-μM samples of SN-OB in 50 mM acetate, pH 4.5, were incubated overnight at 4 °C with varying concentrations of GuHCl. For the refolding transitions (Pace, 1986), unfolded samples of SN-OB in 6 M GuHCl were diluted to varying concentrations of denaturant, and to a final protein concentration of 35 μM. Concentrations of GuHCl (ultrapure, ICN Biomedicals) were determined from refractive index measurements (Pace, 1986).

Acknowledgments: We thank Drs. W. Jahnke and M.J.J. Blommers (Physics, CIBA-Geigy AG, Basel) for discussion and use of their NMR spectrometer. Supported by Swiss National Science Foundation grant 31-43091.95 to A.T.A.

References

Alexandrescu AT, Gittis A, Abeygunawardana C, Shortle D. 1995. NMR structure of a stable "OB-fold" sub-domain isolated from staphylococcal nuclease. *J Mol Biol 250*:134–143.

Antuch W, Güntert P, Billeter M, Hawthorne T, Grossenbacher H, Wüthrich K. 1994. NMR solution structure of the recombinant tick anticoagulant protein (rTAP), a factor Xa inhibitor from the tick *Ornithodos moubata*. *FEBS Lett 352*:251–257.

Bai Y, Milne JS, Mayne L, Englander SW. 1993. Primary structure effects on peptide group hydrogen exchange. *Proteins Struct Funct Genet 17*:75–86.

Bai Y, Sosnick TR, Mayne L, Englander SW. 1995. Protein folding intermediates studied by native-state hydrogen exchange. *Science 269*:192–197.

Baldwin RL. 1993. Pulsed H/D-exchange studies of folding intermediates. *Curr Opin Struct Biol 3*:84–91.

Baldwin RL. 1995. The nature of protein folding pathways: The classical versus the new view. *J Biomol NMR 5*:103–109.

Buck M, Radford SE, Dobson CM. 1994. Amide hydrogen exchange in a highly denatured state. Hen egg-white lysozyme in urea. *J Mol Biol 237*:247–254.

Dolgikh DA, Gilmashin RI, Brazhnikov EV, Bychkova VE, Semisotnov GV, Venyaminov SYu, Ptitsyn OB. 1981. α-Lactalbumin: Compact state with fluctuating tertiary structure? *FEBS Lett 136*:311–315.

Englander SW, Kallenbach NR. 1984. Hydrogen exchange and structural dynamics of proteins and nucleic acids. *Q Rev Biophys 16*:521–655.

Englander SW, Mayne L. 1992. Protein folding studied using hydrogen-exchange labeling and two-dimensional NMR. *Annu Rev Biophys Biomol Struct 21*:243–65.

Guijarro JI, Jackson M, Chaffote AF, Delepierre M, Mantsch HH, Goldberg ME. 1995. Protein folding intermediates with rapidly exchangeable amide protons contain authentic hydrogen-bonded secondary structures. *Biochemistry 34*:2998–3008.

Hughson FM, Wright PE, Baldwin RL. 1990. Structural characterization of a partly folded apomyoglobin intermediate. *Science 249*:1544–1548.

Hynes TR, Fox RO. 1991. The crystal structure of staphylococcal nuclease refined at 1.7 Å resolution. *Proteins Struct Funct Genet 10*:92–105.

Jacobs MD, Fox RO. 1994. Staphylococcal nuclease folding intermediates characterized by hydrogen exchange and NMR spectroscopy. *Proc Natl Acad Sci USA 91*:449–453.

Kalnin NN, Kuwajima K. 1995. Kinetic folding and unfolding of staphylococcal nuclease and its six mutants by stopped-flow circular dichroism. *Proteins Struct Funct Genet 23*:163–176.

Kay LE, Keifer P, Saarinen T. 1992. Pure absorption gradient enhanced heteronuclear single quantum correlation spectroscopy with improved sensitivity. *J Am Chem Soc 114*:10663–10665.

Koide S, Jahnke W, Wright PE. 1995. Measurement of intrinsic exchange rates of amide protons in a ^{15}N-labeled peptide. *J Biomol NMR 6*:306–312.

Kuboniwa H, Tjandra N, Grzesiek S, Ren H, Klee CB, Bax A. 1995. Solution structure of calcium-free calmodulin. *Nature Struct Biol 2*:768–776.

Linderstrøm-Lang K. 1955. Deuterium exchange between peptides and water. *Chem Soc (Lond) Spec Publ 2*:1–20.

Loh SN, Prehoda KE, Wang J, Markley JL. 1993. Hydrogen exchange in unligated and ligated staphylococcal nuclease. *Biochemistry 32*:11022–11028.

Lu J, Dahlquist FW. 1992. Detection and characterization of an early folding intermediate of T4 lysozyme using pulsed hydrogen exchange and two-dimensional NMR. *Biochemistry 31*:4749–4756.

Miranker A, Radford SE, Karplus M, Dobson CM. 1991. Demonstration by NMR of folding domains in lysozyme. *Nature 349*:633–636.

Miranker AD, Dobson CM. 1996. Collapse and cooperativity in protein folding. *Curr Opin Struct Biol 6*:31–42.

Murzin AG. 1993. OB(oligonucleotide/oligosaccharide binding)-fold: Common structural and functional solution for non-homologous sequences. *EMBO J 12*:861–867.

Neri D, Billeter M, Wider G, Wüthrich K. 1992. NMR determination of residual structure in a urea-denatured protein, the 434-repressor. *Science 257*:1559–1563.

Ohgushi M, Wada A. 1983. "Molten-globule state:" A compact form of globular proteins with mobile side-chains. *FEBS Lett 164*:21–24.

Pace CN. 1986. Determination and analysis of urea and guanidine hydrochloride denaturation curves. *Methods Enzymol 131*:266–280.

Pedersen TG, Thomsen NK, Andersen KV, Madsen JC, Poulsen FM. 1993. Determination of the range constants *k1* and *k2* of the Linderstrøm-Lang model for protein amide hydrogen exchange. *J Mol Biol 230*:651–660.

Radford SE, Dobson CM, Evans PA. 1992. The folding of hen lysozyme involves partially structured intermediates and multiple pathways. *Nature 358*:302–307.

Robinson CV, Groβ M, Eyles SJ, Ewbank JJ, Mayhew M, Hartl FU, Dobson CM, Radford SE. 1994. Conformation of GroEL-bound α-lactalbumin probed by mass spectrometry. *Nature 372*:646–651.

Roder H, Elöve G, Englander SW. 1988. Structural characterization of folding intermediates in cytochrome *c* by H-exchange labelling and proton NMR. *Nature 335*:700–704.

Shortle D. 1986. Stability mutants of staphylococcal nuclease: A correlation between nuclease activity in an agar gel assay and stability to guanidine hydrochloride denaturation. In: Inouye M, Sarma R, eds. *Protein engineering: Applications to science, medicine, and industry*. New York: Academic Press. pp 233–241.

Shortle D, Meeker AK. 1986. Mutant forms of staphylococcal nuclease with altered patterns of guanidine hydrochloride and urea denaturation. *Proteins Struct Funct Genet 1*:81–89.

Shortle D, Meeker AK. 1989. Residual structure in large fragments of Staphylococcal nuclease: Effects of amino acid substitutions. *Biochemistry 28*:936–944.

Tjandra N, Kuboniwa H, Bax A. 1995. Rotational dynamics of calcium-free calmodulin studied by ^{15}N-NMR relaxation measurements. *Eur J Biochem 230*:1014–1024.

Udgaonkar JB, Baldwin RL. 1988. NMR evidence for an early framework intermediate on the folding pathway of ribonuclease A. *Nature 335*:694–699.

Wang Y, Shortle D. 1995. The equilibrium folding pathway of staphylococcal nuclease: Identification of the most stable chain–chain interactions by NMR and CD spectroscopy. *Biochemistry 34*:15895–15905.

Zahn R, Spitzfaden C, Ottiger M, Wüthrich K, Plückthun A. 1994. Destabilization of the complete protein secondary structure on binding to the chaperone GroEL. *Nature 368*:261–265.